

GaSb-based type-I quantum well cascade diode lasers emitting at nearly 2-μm wavelength with digitally grown AlGaAsSb gradient layers

Yi Zhang(张一), Cheng-Ao Yang(杨成奥), Jin-Ming Shang(尚金铭), Yi-Hang Chen(陈益航), Tian-Fang Wang(王天放), Yu Zhang(张宇), Ying-Qiang Xu(徐应强), Bing Liu(刘冰), and Zhi-Chuan Niu(牛智川)

Citation: Chin. Phys. B, 2021, 30 (**9**): 094204. DOI: 10.1088/1674-1056/abe930
Journal homepage: http://cpb.iphy.ac.cn; http://iopscience.iop.org/cpb

What follows is a list of articles you may be interested in

An approach to gas sensors based on tunable diode laser incomplete saturated absorption spectra

Wei Nie(聂伟), Zhen-Yu Xu(许振宇), Rui-Feng Kan(阚瑞峰), Mei-Rong Dong(董美蓉), and Ji-Dong Lu(陆继东)
Chin. Phys. B, 2021, 30 (**6**): 064213. DOI: 10.1088/1674-1056/abd769

Analysis of relative wavelength response characterization and its effects on scanned-WMS gas sensing

Dao Zheng(郑道), Zhi-Min Peng(彭志敏), Yan-Jun Ding(丁艳军), and Yan-Jun Du(杜艳君)
Chin. Phys. B, 2021, 30 (**4**): 044210. DOI: 10.1088/1674-1056/abdb1c

High-performance frequency stabilization of ultraviolet diode lasers by using dichroic atomic vapor spectroscopy and transfer cavity

Danna Shen(申丹娜), Liangyu Ding(丁亮宇), Qiuxin Zhang(张球新), Chenhao Zhu(朱晨昊), Yuxin Wang(王玉欣), Wei Zhang(张威), Xiang Zhang(张翔)
Chin. Phys. B, 2020, 29 (**7**): 074210. DOI: 10.1088/1674-1056/ab8c41

High performance GaSb based digital-grown InGaSb/AlGaAsSb mid-infrared lasers and bars

Sheng-Wen Xie(谢圣文), Yu Zhang(张宇), Cheng-Ao Yang(杨成奥), Shu-Shan Huang(黄书山), Ye Yuan(袁野), Yi Zhang(张一), Jin-Ming Shang(尚金铭), Fu-Hui Shao(邵福会), Ying-Qiang Xu(徐应强), Hai-Qiao Ni(倪海桥), Zhi-Chuan Niu(牛智川)
Chin. Phys. B, 2019, 28 (**1**): 014208. DOI: 10.1088/1674-1056/28/1/014208

Laser absorption spectroscopy for high temperature H_2O time-history measurement at 2.55 μm during oxidation of hydrogen

Yu-Dan Gou(苟于单), De-Xiang Zhang(张德翔), Yi-Jun Wang(王易君), Chang-Hua Zhang(张昌华), Ping Li(李萍), Xiang-Yuan Li(李象远)
Chin. Phys. B, 2018, 27 (**7**): 074213. DOI: 10.1088/1674-1056/27/7/074213

GaSb-based type-I quantum well cascade diode lasers emitting at nearly 2-μm wavelength with digitally grown AlGaAsSb gradient layers*

Yi Zhang(张一)[1,2], Cheng-Ao Yang(杨成奥)[1,2], Jin-Ming Shang(尚金铭)[1,2], Yi-Hang Chen(陈益航)[1,2], Tian-Fang Wang(王天放)[1,2], Yu Zhang(张宇)[1,2], Ying-Qiang Xu(徐应强)[1,2], Bing Liu(刘冰)[3], and Zhi-Chuan Niu(牛智川)[1,2,3,†]

[1] *State Key Laboratory for Superlattices and Microstructures, Institute of Semiconductor, Chinese Academy of Sciences, Beijing* 100083, *China*

[2] *College of Materials Science and Optoelectronics Engineering, University of Chinese Academy of Sciences, Beijing* 100049, *China*

[3] *Beijing Academy of Quantum Information Sciences, Beijing* 100193, *China*

(Received 18 November 2020; revised manuscript received 17 February 2021; accepted manuscript online 24 February 2021)

We report a GaSb-based type-I quantum well cascade diode laser emitting at nearly 2-μm wavelength. The recycling of carriers is realized by the gradient AlGaAsSb barrier and chirped GaSb/AlSb/InAs electron injector. The growth of quaternary digital alloy with a gradually changed composition by short-period superlattices is introduced in detail in this paper. And the quantum well cascade laser with 100-μm-wide, 2-mm-long ridge generates an about continuous-wave output of 0.8 W at room temperature. The characteristic temperature T_0 is estimated at above 60 K.

Keywords: antimony, quantum well cascade, diode laser, molecular beam epitaxy

PACS: 42.55.Px, 42.50.–p, 78.55.Cr, 78.67.De **DOI:** 10.1088/1674-1056/abe930

1. Introduction

Mid-infrared high-power semiconductor lasers have received increasingly attention in many fields, such as LIDAR seeding,[1] medical care, surgery, and spectral detection.[2] GaSb-based diode lasers are an ideal light source lasing in mid-infrared band.[3–5] At present, traditional GaSb-based type-I quantum well (QW) laser has been reported to reach more than 1.5-W output power.[6,7] However, the lasers with cascade pumping scheme have also been widely studied because they can significantly increase output power and extend the lasing wavelength. Currently, the type-I QW cascade lasers have achieved higher power of 1.9 W at 2.0 μm and 960 mW at 3 μm.[8,9] And interband cascade laser (ICL) can easily cover the whole spectral range of 3 μm–4 μm.[10–12] The cascade lasers are physically different from conventional QW lasers. For a non-cascade laser, electrons and holes are injected into each quantum well from the PN junction, which connects the multi-quantum wells (MQWs) "in parallel". This causes each electron–hole pair to recombine only once and emit one photon. The cascade QW laser has a cascade region that is composed of GaSb/InAs heterostructure and the several periods' superlattices (SL) of InAs/AlSb injector. The reuse of electrons and holes is realized through this tunneling junction and injection region, which is the same as the ICL with type-II QWs.[13] The cascade structure enables a pair of electron and hole to pass through all MQWs and connects the MQWs "in series", which enables the cyclic electron–hole pair to emit multiple photons.[14] As a result, the cascade structure can reduce the net threshold power density and realize the reuse of the electrons and holes.[15] Besides, the cascade structure has higher internal quantum efficiency in theory.

In 2013, the type-I QW cascade diode laser was reported to reach high output power at 3-μm wavelength and its internal efficiency was about 130% at room temperature which means that the cascade structure provided efficient carrier recycling between stages.[16,17] After that, by eliminating the separation between the active quantum well and the electron injector, the 960-mW output in RTCW at 3-μm wavelength and internal efficiency about 190% of three-stage cascade laser was reported.[12] Then, the same cascade structure was used in 2-μm devices, and high power nearly 2 W has been achieved.[11,18] Recently, the long wavelength LED at 3 μm–3.5 μm with the same structure was also reported.[19]

In this work, we report the structure and fabrication of type-I QW cascade laser. Especially, we introduce the cascade region and the growth of gradually changed composition quaternary alloy with short-period superlattices. Then the fabrication of the quantum well cascade laser is introduced, and nearly 800-mW output of laser at RTCW is obtained.

*Project supported by the Major Program of the National Natural Science Foundation of China (Grant No. 61790581) and the Key Area Research and Development Program of Guangdong Province, China (Grant No. 2020B0303020001).

†Corresponding author. E-mail: zcniu@semi.ac.cn

© 2021 Chinese Physical Society and IOP Publishing Ltd

2. Device epitaxy and structure

A GEN-II molecular beam epitaxy (MBE) is used to grow the type-I QW cascade laser. The solid sources for the group-III elements and group-V arsenic (As) and antimony (Sb) valved cracker cells are installed on the MBE. The Te-doped n-GaSb substrates are thermally deoxidized under Sb_2 stabilization at 600 °C for 20 min. After that, the substrate temperature decreases for better material growth quality. The device structure of the cascade QW laser is shown in Fig. 1. The growth begins with a GaSb buffer layer with a thickness of 300 nm for a flat surface. After the buffer layer, a 2000-nm thick N-type $Al_{0.5}Ga_{0.5}As_{0.05}Sb_{0.95}$ cladding layer with Te-doped (1×10^{17} cm^{-3}) which is matched to the substrate, is grown, followed by the 240-nm-thick waveguide layer of undoped $Al_{0.25}Ga_{0.75}As_{0.02}Sb_{0.98}$. Then the first 13-nm-thick $In_{0.18}Ga_{0.82}Sb$ quantum well (QW1) is grown. And the cascade region is grown to connect the two quantum wells "in series", and the second 13-nm-thick $In_{0.18}Ga_{0.82}Sb$ quantum well (QW2) is grown. The symmetrical structure is was also fabricated which consists of top 240-nm-thick waveguide layer of undoped $Al_{0.25}Ga_{0.75}As_{0.02}Sb_{0.98}$ and top 2000-nm-thick P-type $Al_{0.5}Ga_{0.5}As_{0.05}Sb_{0.95}$ cladding layer with Be atoms (1×10^{18} cm^{-3}) doped. The structure was finished with a GaSb contact layer which is heavily Be-doped (1×10^{18} cm^{-3}) and about 250-nm thick to reduce the contact resistance.

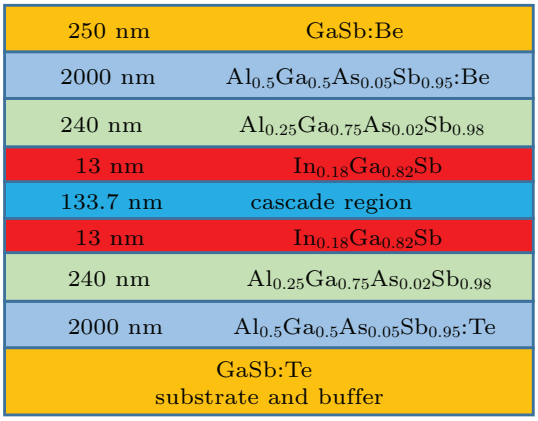


Fig. 1. Full structure of type-I QW cascade laser.

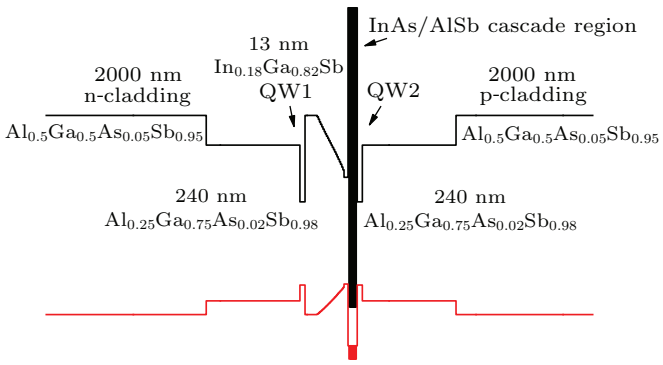


Fig. 2. Band structure of the full structure.

The band structure of the cascade laser in this work is shown in Fig. 2. The cladding layer and waveguide layer are similar to those of the conventional high-power quantum well lasers.[20] For conventional diode laser without cascade structure, there is only a 20-nm barrier between two quantum wells.[21] However, the cascade laser makes some differences between the two QWs.

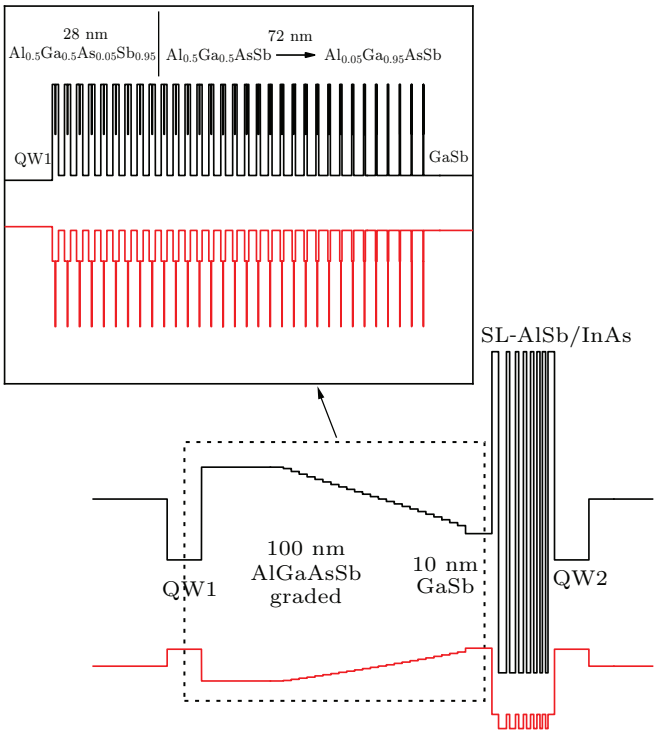


Fig. 3. "Heart" of type-I QW cascade laser and gradient $Al_xGa_{1-x}AsSb$ digital alloy.

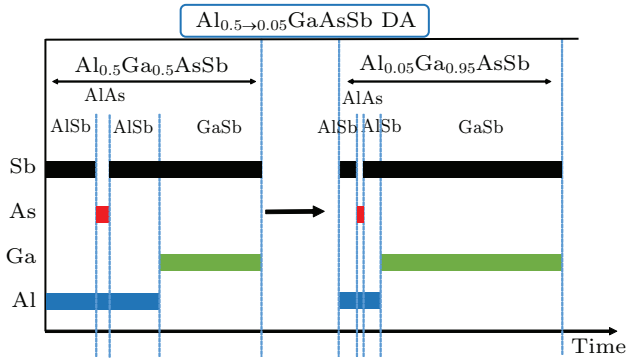


Fig. 4. Shutter sequence of gradient $Al_xGa_{1-x}AsSb$ digital alloy.

The "heart" of the type-I QW cascade laser is shown in Fig. 3. The QW1 is followed by undoped AlGaAsSb with 28-nm-thick $Al_{0.5}Ga_{0.5}As_{0.05}Sb_{0.95}$ and 72-nm-thick graded $Al_xGa_{1-x}AsSb$ layer with x changing from 0.5 to 0.05. The AlGaAsSb graded barrier is used to prevent the electrons from transiting from QW1 to QW2 through the conduction band. The insert in Fig. 3 shows the graded layer with digital alloy. One period of the digital alloys grown by short-period superlattices is about 10 monolayers (MLs) ≈ 3.1 nm. Taking the $Al_{0.5}Ga_{0.5}As_{0.05}Sb_{0.95}$for example, its one period consisting

of 1.44-nm-thick AlSb, 1.52-nm-thick GaSb, and 0.14-nm-thick AlAs is inserted in the AlSb layer to balance the lattice matching. The actual thickness of AlAs is determined by the result of high-resolution x-ray diffraction (HRXRD) to make the digital alloy of $Al_{0.5}Ga_{0.5}As_{0.05}Sb_{0.95}$ matched with the lattice of GaSb substrate. It is identical to growing digital alloy by changing the Al composition. For the gradient $Al_xGa_{1-x}AsSb$, using 10 atomic layers as a cycle, the composition is controlled by adjusting the thickness of AlSb, AlAs, and GaSb, separately.[22,23] The shutter sequence of gradient layer with digital alloys is shown in Fig. 4. For better understanding, the growth times of different composition short period superlattices with different Al compositions of $Al_xGa_{1-x}As_ySb_{1-y}$ digital alloys are shown in Table 1. The growth rates of the group-III elements used here are all 0.5 ML/s. Growing digital alloy gradient layer with short period superlattice is much simpler than directly changing the temperature of the group-III sources to grow random alloy, and growing the random alloys requires the simultaneous controlling of group-V elements to adjust strain which is a little complex. However, the digital alloy only needs to control the shutter to determine the composition. To some extent, it reduces the instability of changing the source temperature and the uncertainty of strain control.

The tunnel junction and the electron injector are followed which connected QW1 and QW2 in series rather than in parallel as shown in Fig. 3. The electrons in the valence band will pass through the GaSb/AlSb/InAs tunnel junction (also called semimetallic interface in ICL) to realize the tunneling from the valence band to the conduction band and the electrons will be injected into the QW2 through the miniband of InAs/AlSb SL electron injector. The tunnel junction consists of 10-nm-thick GaSb, 2.5-nm-thick AlSb, 3-nm-thick InAs, and 1.2-nm-thick AlSb. And the electron injector is comprised of Si-doped (5×10^{17} cm^{-3}) 6-period InAs/AlSb chirped SLs. The layer structure of SLs is as follows: 2.2 nm-thick InAs/1.2-nm-thick AlSb/1.8-nm-thick InAs/1.2-nm-thick AlSb/1.5-nm-thick InAs/1.2-nm-thick AlSb/1.2-nm-thick InAs/1.2-nm-thick AlSb/0.9-nm-thick InAs/1.2-nm-thick AlSb/0.9-nm-thick InAs/2.5-nm-thick AlSb. Then the second quantum well (QW2) of 13-nm-thick $In_{0.18}Ga_{0.82}Sb$ is grown.

Table 1. Growth times of AlSb/AlAs/AlSb/GaSb short-period superlattices with different compositions of $Al_xGa_{1-x}As_ySb_{1-y}$ digital alloys.

Al composition x	As composition y	AlSb (s)	AlAs (s)	AlSb (s)	GaSb (s)
0.50	0.0435	4.68	0.99	4.68	9.99
0.49	0.0427	4.42	0.96	4.42	10.20
0.47	0.0410	4.24	0.93	4.24	10.60
...					
0.09	0.0081	0.78	0.24	0.78	18.20
0.07	0.0063	0.60	0.21	0.60	18.60
0.05	0.0045	0.42	0.17	0.42	19.00

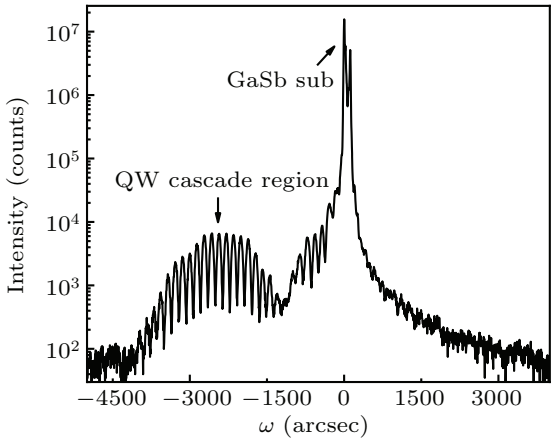


Fig. 5. HRXRD spectrum of type-I QW cascade laser with QW cascade region marked.

Figure 5 shows the HRXRD curve of the quantum well cascade laser. The central peak for the $Al_{0.5}Ga_{0.5}As_{0.05}Sb_{0.95}$ cladding layer and the $Al_{0.25}Ga_{0.75}As_{0.02}Sb_{0.98}$ waveguide layer coincide with the substrate peak, indicating that the lattice of material matches with that of the substrate, and the clear satellite peak of QW cascade region indicates the high growth quality of the material.

3. Laser performance

By lithographing and inductively coupled plasma etching (ICP), the 2-mm-long 100-μm-wide strip ridges are fabricated. And 250-nm-thick Si_3N_4 films are deposited for insulation by the plasma-enhanced chemical vapor deposition (PECVD). Then the p-contact electrode Ti/Pt/Au is formed by sputtering. With the substrate thinned by chemical mechanical polishing (CMP) technique, the n-contact is achieved by sputtering AuGeNi/Au and rapid thermal process (RTP). After cleaving into 2-mm-long chips, Al_2O_3 anti-reflection (AR $< 5\%$) and high-reflection 2-pairs Si/SiO_2 (HR $> 95\%$) are coated. The devices were all epi-side down, and the light–current–voltage characteristics for 100-μm-wide, 2-mm-long coated QW cascade laser in continuous wave at different temperatures are shown in Fig. 6.

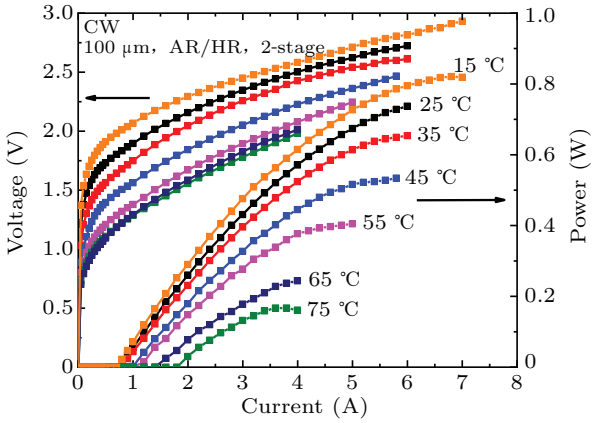


Fig. 6. The *L–I–V* for 100-μm-wide, 2-mm-long coated lasers in continuous wave at different temperatures.

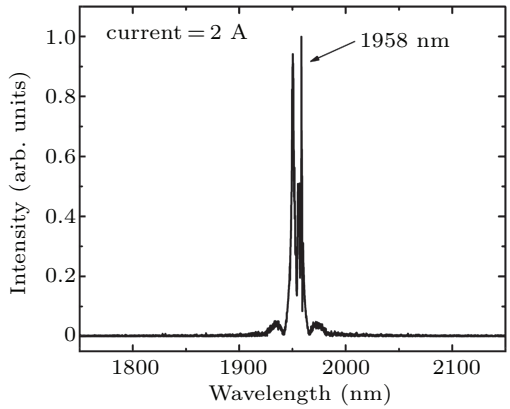


Fig. 7. Spectrum of room-temperature quantum-well cascade continuous-wave laser at 2 A.

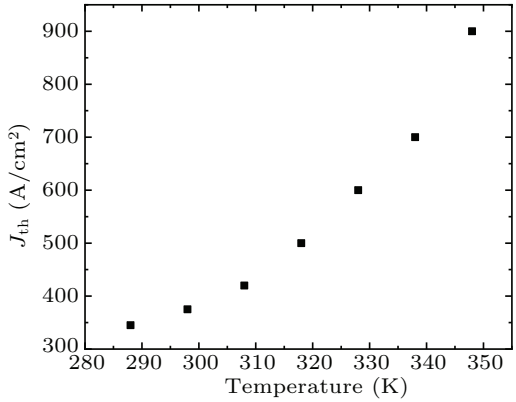


Fig. 8. Variations of threshold current densities with temperatures.

The threshold current density of $J_{th} = 345$ A/cm^2 and the maximum output power 800 mW at 15 °C are achieved. The slope efficiency is estimated at 200 mW/A. The internal efficiency of the 100-μm wide two-stage cascade laser is ∼ 105% at room temperature which confirms the recycling process of carriers. The direct electron tunneling from QW1 to QW2 can be reduced by increasing the Al composition of the AlGaAsSb gradient layer and doping with Be. And by adjusting the energy levels in InAs/AlSb injector, the internal quantum efficiency can be improved. The emission spectra are measured by a Fourier-transform infrared (FTIR) method and figure 7 shows the laser spectrum of laser at 2 A at room temperature whose wavelength is near 1950 nm. Temperature dependence of J_{th} in CW coated laser is shown in Fig. 8. Through calculation, the characteristic temperature $T_0 \approx 62$ K.

4. Conclusions and perspectives

In this work, we report the AlGaAsSb quaternary digital alloy with the short period superlattices, fabricated by molecular beam epitaxy. The GaSb-based quantum well cascade laser is emitted at about 2 μm, and reaches nearly 800-mW output power. The characteristic temperature is $T_0 \approx 62$ K. We believe that the cascade structure will become more effective and have better device performance, by increasing the Al composition of gradient AlGaAsSb and changing the band structure of InAs/AlSb electron injector to change energy.

References

[1] Forouhar S, Briggs R M, Frez C, Franz K J and Ksendzov A 2012 *Appl. Phys. Lett.* **100** 031107
[2] Rothman L S, Gordon I E, Babikov Y, Barbe A and Wagner G 2013 *J. Quantum Spec. Radi. Transfer* **130** 4
[3] Pfahler C, Kaufel G, Kelemen M T, Mikulla M, Rattunde M, Schmitz J and Wagner J 2006 *IEEE Photon. Technol. Lett.* **18** 758
[4] Kim J G, Shterengas L, Martinelli R U, Belenky G L and Chan W K 2002 *Appl. Phys. Lett.* **81** 3146
[5] Shterengas L, Belenky G, kipshidze G and Hosoda T 2008 *Appl. Phys. Lett.* **92** 171111
[6] Chen J, Kipshidze G and Shterengas L 2010 *IEEE J. Quantum Electron* **46** 1464
[7] Xie S W, Yang C A, Huang S S, Yuan Y and Niu Z C 2019 *Super. Micro.* **130** 339
[8] Hosoda T, Feng T, Shterengas L, Kipshidze G and Belenky G 2016 *Appl. Phys. Lett.* **108** 131109
[9] Shterengas L, Liang R, Kipshidze G, Hosoda T, Belenky G, Bowman S S and Tober R L 2014 *Appl. Phys. Lett.* **105** 161112
[10] Canedy C L, Abell J, Merritt C D, Bewley W W, Kim C S, Kim M, Vurgaftman I and Meyer J R 2014 *Opt. Express* **22** 7702
[11] Zhang Y, Shao F H, Yang C A, Xie S W, Huang S S, Yuan Y, Shang J M, Zhang Y, Xu Y Q and Niu Z C 2018 *Chin. Phys. B* **27** 124207
[12] Canedy C L, Warren M V, Merritt C D, Bewley W W, Kim C S, Kim M, Vurgaftman I and Meyer J R 2017 *Proc. SPIE* **10111** 10111
[13] Vurgaftman I, Bewley W W, Canedy C L, Kim C S, Kim M, Merritt C D, Abell J, Lindle J R and Meyer J R 2011 *Nat. Commun.* **2** 585
[14] Yang R Q and Pei S S 1996 *J. Appl. Phys.* **79** 8197
[15] Vurgaftman I, Bewley W W, Canedy C L, Kim C, Kim M, Lindle J J, Merritt C D, Abell J and Meyer J R 2011 *IEEE J. Sel. Top. Quantum Electron.* **17** 1435
[16] Shterengas L, Liang R, Kipshidze G, Hosoda T, Suchalkin S and Belenky G 2013 *Appl. Phys. Lett.* **103** 121108
[17] Shterengas L, Liang R, Kipshidze G and Belenky G 2014 *Proc. SPIE* **9002** 900213
[18] Shterengas L, Kipshidze G, Hosoda T, Liang R, Feng T, Wang M, Aaron S and Belenky G 2017 *IEEE J. Select. Top. Quantum Electron.* **23** 1500708
[19] Ermolaev M, Lin Y X, Shterengas L, Hosoda T and Belenky G 2018 *IEEE Photon. Technol. Lett.* **30** 869
[20] Xie S W, Zhang Y, Yang C A, Huang S S, Yuan Y, Zhang Y, Shang J M, Shao F H, Xu Y Q and Niu Z C 2019 *Chin. Phys. B* **28** 014208
[21] Liang R, Chen J, Kipshidze G, Westerfeld D, Shterengas L and Belenky G 2011 *IEEE Photon. Technol. Lett.* **23** 603
[22] Mahalingam K, Haugan H J, Brown G J and Aronow A J 2013 *Appl. Phys. Lett.* **103** 211605
[23] Maddox S J, March S D and Bank S R 2016 *Cryst. Growth Des.* **16** 3582